Inorganic Chemistry
Article

Inorg. Chem. **2011**, *50*, 1689–1697 **1689**
DOI: 10.1021/ic102173f

Nonmacrocyclic Luminescent Lanthanide Complexes Stable in Biological Media

Nchimi Nono Katia,[†] Alexandre Lecointre,[†] Martín Regueiro-Figueroa,[‡] Carlos Platas-Iglesias,[‡] and Loïc J. Charbonnière*,[†]

[†]*Laboratoire d'Ingénierie Moléculaire Appliquée à l'Analyse, IPHC, UMR 7178 CNRS/UdS, ECPM, Bâtiment R1N0, 25 Rue Becquerel, 67087, Strasbourg Cedex 02, France, and* [‡]*Departamento de Química Fundamental, Universidade da Coruña, Campus de Zapateira, Rúa da Fraga 10, 15008, A Coruña, Spain*

Received October 28, 2010

The synthesis of ligand $\mathbf{L_P}H_8$, based on a 2,6-bispyrazolyl-pyridine scaffold functionalized by iminobismethylenephosphonate functions, is described and its p*K* values were determined by a combination of pH-spectrophotometric titrations and potentiometry. The interaction of $\mathbf{L_P}$ with Tb^{3+} was investigated in water (0.01 M TRIS/HCl pH = 7.0) by means of UV−vis and fluorescence titration experiments and evidenced the formation of at least three species with 1:1; 1:2, and 2:1 M−L ratios, the 1:1 complex appearing as particularly stable under these conditions (log K_{cond} > 8). $Na_4[Ln\mathbf{L_P}H]$ complexes (Ln = Eu and Tb) were prepared and characterized by elemental analysis, IR spectroscopy, and electrospray mass spectrometry. Their photophysical properties were investigated in aqueous solutions, revealing an excellent shielding of the Ln cations from the solvent environment (no water molecules in the first coordination sphere), very long luminescence lifetimes (τ_{H_2O} = 1.50 and 3.28 ms, respectively, for Eu and Tb) and reasonable luminescent quantum yields (ϕ_{H_2O} = 2.4 and 37%, respectively, for Eu and Tb). Using fetal bovine serum as a model for biological media showed the Tb complex to remain luminescent in these conditions. The structure of the europium complex was studied by means of density functional theory (DFT) modeling, confirming the wrapping of the ligand around the cation, and the very good shielding of the coordinated Ln cation. The conditional stability constant for the formation of the Tb complex with $\mathbf{L_P}$ was determined by competition experiments with EDTA and monitored by fluorescence spectroscopy (log $K_{Tb\mathbf{L_P}}$cond = 14.1 ± 0.3, 0.01 M TRIS/HCl, pH = 7.4) and was used to determine the thermodynamic constant (log $K_{Tb\mathbf{L_P}}$ = 20.4 ± 0.4). A systematic comparison with ligand $\mathbf{L_C}$, in which phosphonate functions are replaced by carboxylate ones, is made throughout the study, highlighting the large interest of the introduction of phosphonate moieties to obtain biologically stable luminescent lanthanide complexes.

Introduction

Thanks to their exceptional photophysical properties,[1,2] luminescent lanthanide complexes have carved out their niche in bioanalytical applications.[3−6] However, the design of highly luminescent lanthanide complexes and labels for biological applications often remains a synthetic challenge that must combine the introduction of adequate chromophoric units, *sine qua non* condition to a high luminescence efficiency, and an adapted ligand scaffold that affords stable complexes, even in aggressive biological media such as sera that contain numerous anionic and cationic competitors. Up until now, the majority of complexes displaying sufficient biological stability for *in vitro* biological applications are obtained from macrocyclic ligands,[7] most often based on a cyclen,[8] macrobicyclic ones such as the famous europium cryptands reported by Lehn,[9] or by self-assembly processes leading to dinuclear triple stranded lanthanide complexes.[10] The architectural design of macrocyclic structures decreases

*E-mail: l.charbonn@unistra.fr.

(1) (a) Bünzli, J.-C. G.; Piguet, C. *Chem. Soc. Rev.* **2005**, *34*, 1048. (b) Yam, V. W.-W.; Lo, K. K.-W. *Coord. Chem. Rev.* **1998**, *184*, 157. (c) Parker, D.; Dickins, R. S.; Puschmann, H.; Crossland, C.; Howard, J. A. K. *Chem. Rev.* **2002**, *102*, 1977. (d) de Bettencourt-Dias, A. *Curr. Org. Chem.* **2007**, *11*, 1460.
(2) (a) Hemmillä, I. *J. Alloys Compd.* **1995**, *225*, 480. (b) Charbonnière, L. J.; Weibel, N.; Estournes, C.; Leuvrey, C.; Ziessel, R. *New J. Chem.* **2004**, *28*, 777.
(3) Selvin, P. R. *Annu. Rev. Biophys. Biomol. Struct.* **2002**, *31*, 275.
(4) (a) Song, B.; Vandevyver, C. D. B.; Chauvin, A. S.; Bünzli, J.-C. G. *Org. Biomol. Chem.* **2008**, *6*, 4125. (b) Shao, G.; Han, R.; Ma, Y.; Tang, M.; Xue, F.; Sha, Y.; Wang, Y. *Chem.—Eur. J.* **2010**, *16*, 8647.
(5) (a) Tsukube, H.; Shinoda, S. *Chem. Rev.* **2002**, *102*, 2389. (b) Dos Santo, C. M. G.; Gunnlaugsson, T. *Dalton Trans.* **2009**, 4712. (c) Parker, D. *Coord. Chem. Rev.* **2000**, *205*, 109. (d) Mameri, S.; Charbonnière, L. J.; Ziessel, R. F. *Inorg. Chem.* **2004**, *43*, 1819.
(6) (a) Bünzli, J.-C. G. *Chem. Rev.* **2010**, *110*, 2729. (b) Geissler, D.; Charbonnière, L. J.; Ziessel, R. F.; Butlin, N. G.; Löhmannsröben, H.-G.; Hildebrandt, N. *Angew. Chem., Int. Ed.* **2010**, *49*, 1396. (c) Mathis, G. *Clin. Chem.* **1995**, *41*, 1391.
(7) (a) Law, G. L.; Pal, R.; Palsson, L. O.; Parker, D.; Wong, K.-L. *Chem. Commun.* **2009**, 7321. (b) D'Aléo, A.; Xu, J.; Do, K.; Muller, G.; Raymond, K. N. *Helv. Chim. Acta* **2009**, *92*, 2439.
(8) Natrajan, L. S.; Villaraza, A. J. L.; Kenwright, A. M.; Faulkner, S. *Chem. Commun.* **2009**, *40*, 6020.
(9) Alpha, B.; Lehn, J.-M.; Mathis, G. *Angew. Chem., Int. Ed.* **1987**, *26*, 266.

Chart 1. Ligands Discussed in the Present Work

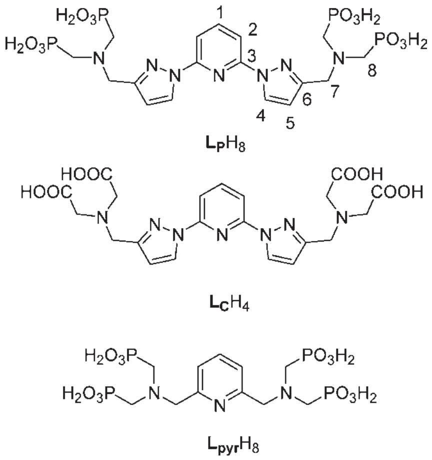

the conformational freedom to ensure stability, but it also drastically limits the synthetic strategies for introduction of the absorbing chromophoric units. An alternative to achieve high thermodynamic stabilities with nonmacrocyclic structures resides in the introduction of anionic functions having strong affinity for Ln^{3+} cations such as carboxylate and phophonate anions. The latter groups have been shown to provide increased stability in aqueous solutions[11] compared to carboxylate analogues but also to increase steric hindrance around the Ln cation,[12] thereby decreasing the interactions with solvent molecules, a particularly important point regarding the luminescence quenching effect of water.[13] In an effort to further develop this approach, we synthesized ligand $\mathbf{L_P}H_8$ (Chart 1), containing a bispyrazolylpyridyl chromophoric unit functionalized with two bis(methylenephosphonate)aminomethyl arms.

Previous investigations showed that depending on the para functionalization of the central pyridyl ring, the bispyrazolylpyridyl chromophore of ligand $\mathbf{L_C}H_4$ (Chart 1) provides a good to excellent energy transfer to the Ln cations, particularly for Tb^{3+}.[14,15] The present work aims at revealing the influence of the replacement of carboxylic units by phosphonate ones, on the spectroscopic, structural, and thermodynamic properties of the corresponding lanthanide complexes. The ligand protonation constants were obtained by using a combination of pH potentiometry and spectrophotometric titrations. The formation of the complexes in aqueous solution was monitored by using both absorption and emission spectroscopies, and the photophyscial properties of the 1:1 (Ln:L) complexes were investigated in detail. Density functional theory (DFT) calculations were used to obtain information on the structure of the complexes in aqueous solution. Finally, the thermodynamic stability of the complexes was assessed by using a competitive luminescence assay with EDTA.

Results and Discussion

Synthesis of the Ligand. Ligand $\mathbf{L_P}H_8$ was obtained in two synthetic steps by using a N-alkylation reaction of 2,6-bis(3-bromomethylpyrazolyl)pyridine, **1**,[14] with tetraethyliminobis(methanephosponate), obtained by literature procedure,[16] to afford the octaethyl ester precursor **2** in 58% chemical yield after purification. Compound **2** was subjected to an acidic hydrolysis of the phosphonic esters with HCl to give the desired ligand with an overall yield of 52% (Scheme 1).

Determination of Protonation Constants of the Ligand. The protonation constants of the ligand were determined by a combination of UV−vis vs pH titration experiment and pH-potentiometry. The values of the protonation constants ($K_{\mathbf{LPH}x}$) of $\mathbf{L_P}^{8-}$, the fully deprotonated ligand, obtained in water (0.1 M KCl) are summarized in Table 1, together with the values reported in the literature for ligand $\mathbf{L_C}$,[17] the analogue of $\mathbf{L_P}$ containing carboxylate functions in place of phosphonate ones, and for $\mathbf{L_{pyr}}$ (2,6-bis[(*N*,*N*-bis(methylenephosphonic acid)aminomethyl],[18] whose structure is similar to that of $\mathbf{L_P}$ but without the pyrazolyl rings. A pH-potentiometric titration of the ligand over the pH range 2−12 gave accurate values for the second (9.17), third (6.87), fourth (5.81), fifth (4.75), and sixth (1.48) protonation constants. However, the first protonation constant was too high to be accurately determined by potentiometry. Thus, the first protonation constant of the ligand was estimated by monitoring the changes observed in the absorption spectrum as a function of pH (see Figure S1, Supporting Information). The absorption spectrum of the ligand recorded at pH 13.5 (0.1 KCl) shows three maxima at ∼306, 270, and 249 nm. With a decrease in the pH, the intensity of the bands at 246 and 306 nm decreases, while that of the band at 270 nm increases. A plot of the relative intensity of the bands at ∼246 and 306 nm allowed us to calculate a log K_H value of 11.82 for the first protonation process of the ligand.

For $\mathbf{L_P}$, the data evidenced the presence of two strong acidic sites, attributed in our case to the two tertiary amines by comparison with literature data.[18,19] The four following protonation constants were attributed to the first protonation of each of the phosphonate moieties. As previously observed,[20,21] the replacement of acetate groups

(10) (a) Fernandez-Moreira, V.; Song, B.; Sivagnanam, V.; Chauvin, A.-S.; Vandevyver, C. D. B.; Gijs, M.; Hemmilä, I.; Lehrd, H.-A.; Bünzli, J. C. G. *Analyst* **2010**, *135*, 42. (b) Eliseeva, S. V.; Bünzli, J.-C. G. *Chem. Soc. Rev*. **2010**, *39*, 189.
(11) (a) Comby, S.; Imbert, D.; Chauvin, A. S.; Bünzli, J.-C. G.; Charbonnière, L. J.; Ziessel, R. *Inorg. Chem*. **2004**, *43*, 7369. (b) Chauvin, A.-S.; Comby, S.; Baud, M.; De Piano, C.; Duhot, C.; Bünzli, J.-C. G. *Inorg. Chem*. **2009**, *48*, 10687.
(12) Aime, S.; Gianolo, E.; Corpillo, D.; Cavalotti, C.; Palmisano, G.; Sisti, M.; Giovenzana, G. B.; Pagliarin, R. *Helv. Chim. Acta* **2003**, *86*, 615.
(13) (a) Supkowski, R. M.; Horrocks, W. D. W., Jr. *Inorg. Chim. Acta* **2002**, *340*, 44. (b) Beeby, A.; Clarkson, I. M.; Dickins, R. S.; Faulkner, S.; Parker, D.; Royle, L.; de Sousa, A. S.; Williams, J. A. G.; Woods, M. *J. Chem. Soc., Perkin Trans. 2* **1999**, 493.
(14) (a) Brunet, E.; Juanes, O.; Sedano, R.; Rodriguez-Ubis, J.-C. *Photochem. Photobiol. Sci*. **2002**, *1*, 613. (b) Remuinan, M. J.; Roman, H.; Alonso, M. T.; Rodriguez-Ubis, J.-C. *J. Chem. Soc. Perkin Trans. 2* **1993**, 1099. (c) Brunet, E.; Juanes, O.; Rodriguez-Ubis, J.-C. *Curr. Chem. Biol*. **2007**, *1*, 11.
(15) Kadjane, P.; Starck, M.; Camerel, F.; Hill, D.; Hildebrandt, N.; Ziessel, R.; Charbonnière, L. J. *Inorg. Chem*. **2009**, *48*, 4601.
(16) Aime, S.; Botta, M.; Garino, E.; Crich, S. G.; Giovenzana, G.; Pagliarin, R.; Palmisano, G.; Sisti, M. *Chem.—Eur. J*. **2000**, *6*, 2609.
(17) Mato-Iglesias, M.; Rodriguez-Blas, T.; Platas-Iglesias, C.; Starck, M.; Kadjane, P.; Ziessel, R.; Charbonnière, L. *Inorg. Chem*. **2009**, *48*, 1507.
(18) Abada, S.; Lecointre, A.; Elhabiri, M.; Charbonnière, L. J. *Dalton Trans*. **2010**, *39*, 9055.
(19) (a) Lukes, I.; Kotek, J.; Vojtisek, P.; Hermann, P. *Coord. Chem. Rev*. **2001**, *216*−*217*, 287. (b) Geraldes, C. F. G. C.; Sherry, D. A.; Cacheris, W. P. *Inorg. Chem*. **1989**, *28*, 3336. (c) Guerra, K. P.; Delgado, R.; Lima, L. M. P.; Drew, M. G. B.; Félix, V. *Dalton Trans*. **2004**, 1812.
(20) Burai, L.; Ren, J.; Kovacs, Z.; Brucher, E.; Sherry, A. D. *Inorg. Chem*. **1998**, *37*, 69.

Scheme 1. Synthesis of Ligand $\mathbf{L_P}H_8$[a]

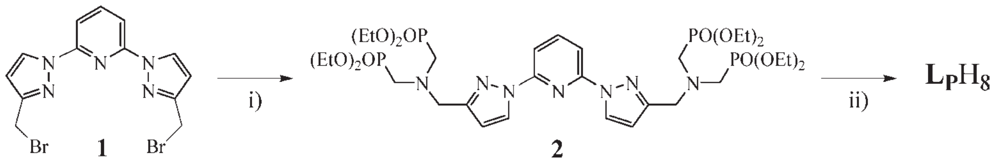

[a] (i) $HN(CH_2PO(OEt)_2)_2$,[16] K_2CO_3, CH_3CN, reflux, 48 h, 58%. (ii) 6 N HCl, 100 °C, 24 h, 90%.

Table 1. Protonation Constants of $\mathbf{L_P}$, $\mathbf{L_C}$,[17] and $\mathbf{L_{Pyr}}$[18] (25 °C, 0.1 M KCl)

	$\mathbf{L_P}$	$\mathbf{L_C}$[17]	$\mathbf{L_{pyr}}$[18]
log K_{LH}	11.82(5)	9.42	11.21
log K_{LH_2}	9.17(2)	7.96	10.29
log K_{LH_3}	6.87(4)	2.70	8.04
log K_{LH_4}	5.81(4)	2.02	6.49
log K_{LH_5}	4.75(5)		5.53
log K_{LH_6}	1.48(5)		4.19

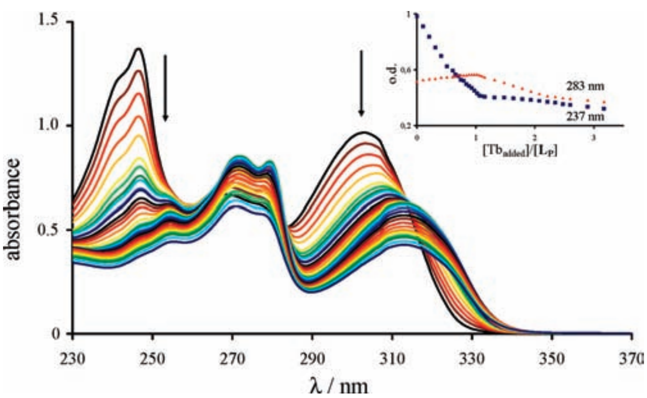

Figure 1. Evolution of the UV−vis absorption spectra of $\mathbf{L_P}$ (c = 4.69 × 10^{-5} M, TRIS/HCl 0.01 M at pH 7.0) upon addition of increasing amounts of $TbCl_3 \cdot 6H_2O$ (uncorrected for dilution). Inset: evolution of the absorbances at 237 and 283 nm.

of the ligand by aminomethylphosphonate ones leads to an important increase in the basicity of the amine nitrogen atoms. In the case of $\mathbf{L_P}$, the presence of the two negative charges of the PO_3^{2-} moiety increases the values of the first and second protonation constants in more than one log unit with respect to the carboxylated compound $\mathbf{L_C}$. A similar situation is observed when comparing the first and second protonation constants of $\mathbf{L_{pyr}}$ and those of the analogue containing carboxylate groups.[18,22]

Spectrophotometric Titration of the Ligand by Tb^{3+}. In order to follow the interaction of the ligand in the presence of lanthanide cations, spectrophotometric titrations of the ligand were performed and monitored by UV−vis absorption and fluorescence emission spectroscopy.

Figure 1 displays the evolution of the absorption spectra as a function of added Tb^{3+} in water (0.01 M TRIS/HCl, pH = 7.0). Upon addition of Tb, the strong absorption band with maximum at 247 nm gradually and continuously decreased in intensity. The absorption band pointing at 303 nm is also decreasing but slowly displaced to lower energy, with a maximum at 315 nm for 1 equiv of Tb. In contrast, the band of medium intensity at 267 nm with a shoulder at 275 nm for the free ligand is slowly increasing up to 1 equiv and the splitting becomes marked, with two contributions at 272 and 279 nm, a characteristic feature of coordinated pyrazolyl compounds.[23] The observation of the evolution of the optical density as a function of the metal/ligand ratio (inset in Figure 2) clearly showed the formation of at least three new species, which was further confirmed by an evolving factor analysis performed with the Specfit software.[24] Regarding the inflection points observed during the titration experiment, the evolution of the spectra was fitted according to a model taking into account the formation of the following species (charges are omitted for the sake of clarity):

$$\mathrm{Tb} + \mathbf{L_P} \leftrightarrow \mathrm{Tb}\mathbf{L_P} \quad \beta_{11} = [\mathrm{Tb}\mathbf{L_P}]/([\mathrm{Tb}][\mathbf{L_P}])$$

$$2\mathrm{Tb} + \mathbf{L_P} \leftrightarrow \mathrm{Tb_2}\mathbf{L_P} \quad \beta_{21} = [\mathrm{Tb_2}\mathbf{L_P}]/([\mathrm{Tb}]^2[\mathbf{L_P}])$$

$$\mathrm{Tb} + 2\mathbf{L_P} \leftrightarrow \mathrm{Tb}\mathbf{L_{P2}} \quad \beta_{12} = [\mathrm{Tb_3}\mathbf{L_{P2}}]/([\mathrm{Tb}][\mathbf{L_P}]^2)$$

Convergence could not be obtained with the proposed species, variations around the inflection points being too marked. This phenomenon can typically be understood on the basis of the formation of very strong complexes (log K > 8), which is obviously the case here. Nevertheless, with large values fixed for β_{11} and K_{21}, it was possible to converge to significant values of the calculated spectra of the species formed, which are presented in Figure 2.

The same titration experiment was followed by fluorescence spectroscopy, monitoring the Tb emission in the 450−700 nm region upon excitation at 300 nm. The results of the fitting are essentially the same as those obtained by absorption spectroscopy, confirming the formation of the three new species, with a very large constant for the 1:1 complex, as evidenced by the steep inflection point obtained at 1 equiv of added Tb (Figure 3).

Synthesis and Spectroscopic Characterization of the $\mathrm{Ln}\mathbf{L_P}$ Complexes. The $\mathrm{Ln}\mathbf{L_P}$ complexes were then prepared by mixing equimolar amounts of the ligand and hydrated lanthanide chloride salts (Ln = La, Eu, and Tb) followed by heating for a few hours before neutralization of the solution and precipitation of the complexes. The

(21) Mato-Iglesias, M.; Balogh, E.; Platas-Iglesias, C.; Toth, E.; de Blas, A.; Rodriguez-Blas, T. *Dalton Trans.* **2006**, 5404.
(22) Pellegatti, L.; Zhang, J.; Drahos, B.; Villette, S.; Suzenet, F.; Guillaumet, G.; Petoud, S.; Toth, E. *Chem. Commun.* **2008**, 6591.
(23) Kadjane, P.; Charbonnière, L.; Camerel, F.; Lainé, P. P.; Ziessel, R. *J. Fluoresc.* **2008**, *18*, 119.
(24) (a) Gampp, H.; Maeder, M.; Meyer, C. J.; Zuberbühler, A. D. *Talanta* **1985**, *32*, 95. (b) Gampp, H.; Maeder, M.; Meyer, C. J.; Zuberbühler, A. D. *Talanta* **1985**, *32*, 251. (c) Gampp, H.; Maeder, M.; Meyer, C. J.; Zuberbühler, A. D. *Talanta* **1986**, *33*, 943.

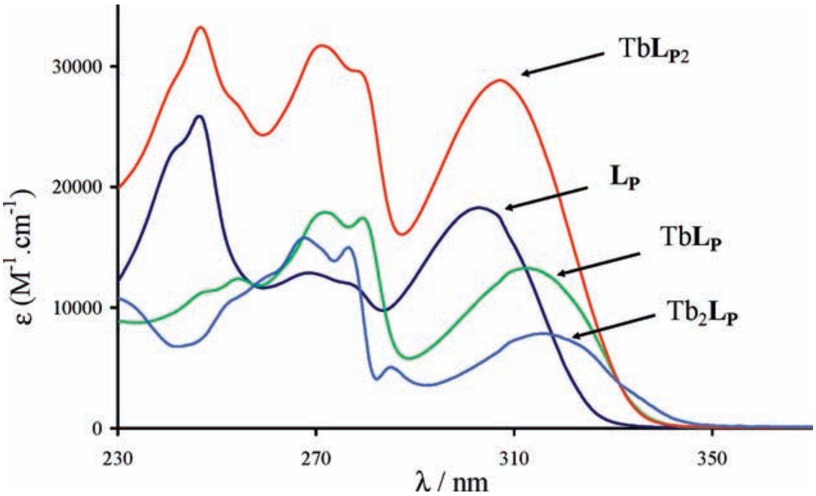

Figure 2. Calculated UV−vis absorption spectra of the species formed during the titration of $\mathbf{L_P}$ by $TbCl_3 \cdot 6H_2O$ in 0.01 M TRIS/HCl pH 7.0.

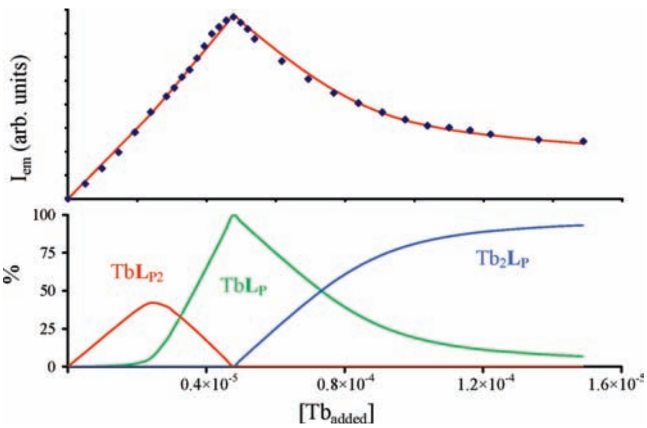

Figure 3. Top: Evolution of the intensity measured at 545 nm (squares, λ_{exc} = 300 nm) upon addition of $TbCl_3$ to a 5.28×10^{-5} M solution of $\mathbf{L_P}$ in water (TRIS/HCl, 0.01 M, pH = 7.0) and the corresponding fitted values (red line). Bottom: evolution of the relative amounts of the species formed during the titration.

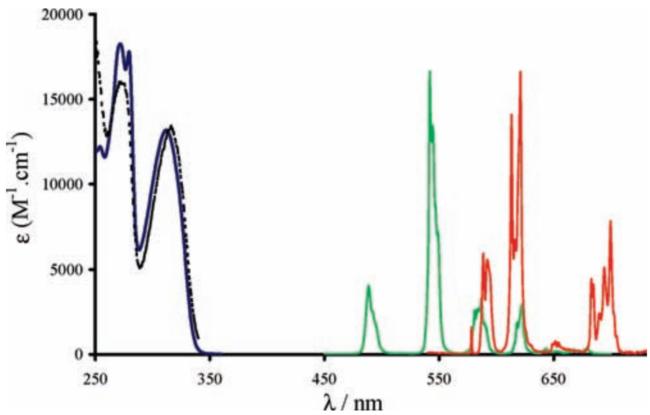

Figure 4. UV−vis absorption (blue), excitation (dashed, λ_{em} = 545 nm), and emission (green, λ_{exc} = 300 nm) spectra of $Na_4[Tb\mathbf{L_P}H]$ and emission spectrum of $Na_4[Eu\mathbf{L_P}H]$ (red, λ_{exc} = 300 nm) in 0.01 M TRIS/HCl, pH = 7.0. (Emission spectra are normalized at their maxima of emission.)

isolated complexes were characterized by elemental analysis, infrared spectroscopy, and mass spectrometry. The latter revealed the presence of major species corresponding to a 1:1 M−L ratio, and in the case of europium, having ^{151}Eu and ^{153}Eu as the two major isotopes, the isotopic distributions pointed to a $[Eu\mathbf{L_P}H_4]^-$ complex (Figure S2, Supporting Information). Interestingly, the spectra of both Eu and Tb complexes displayed 5 main peaks corresponding to the $Na_x[Ln\mathbf{L_P}H_{4-x}]^-$ species with x varying from 0 to 4 (Figures S2 and S3 in the Supporting Information, respectively, for Eu and Tb). The ^{1}H NMR spectrum of the diamagnetic La complex (obtained from a 1:1, $\mathbf{L_P}$−$LaCl_3$ mixture in D_2O at 500 MHz, 298 K, pD = 10.5, see Figure S4 in the Supporting Information) shows the signals of the pyrazolyl groups at 8.36 (H4) and 6.53 ppm (H5), while those of the pyridyl protons are observed as the expected triplet and doublet signals at 8.11 (H1) and 7.55 (H2) ppm (^3J = 7.9 Hz, see Chart 1 for labeling). The CH_2 protons give broad signals at 2.99 (H7) and 4.30 (H8) ppm, which points to a fast interconversion between the Δ and Λ enantiomeric forms of the complex as a consequence of exchange between in-plane and out-of-plane methylenephosphonate groups.[17]

This is confirmed by the ^{13}C NMR spectrum, which shows 8 signals for the 17 carbon nuclei of the ligand backbone [158.3 (C6), 145.1 (C1), 150.4 (C3), 132.0 (C4), 109.1 (C2), 110.0 (C5), 60.7 (C8), and 57.6 ppm (C7)]. As expected, the signal of the $-CH_2-PO_3^{2-}$ carbon (C8) is split into a doublet due to coupling to the ^{31}P nucleus ($^1J_{CP}$ = 142 Hz).[25] The ^{31}P−{^{1}H} spectrum presents a single resonance at 18.8 ppm (Figure S4 in the Supporting Information), thereby confirming that the four methylenephosphonate groups are equivalent, in line with a fast interconversion between the Δ and Λ enantiomeric forms of the complex.

Figure 4 displays the UV−vis absorption, emission, and excitation spectra of the Tb complex and the emission spectrum of the Eu complex in water (pH = 7.0, TRIS/HCl 0.01 M), while the main spectroscopic parameters for the Eu and Tb complexes are presented in Table 2.

Upon complexation of the cation, the main absorption bands of the ligands are bathochromically shifted, as previously observed during the titration experiment. This behavior is typically observed in polypyridyl compounds

(25) Kalman, F. K.; Baranyai, Z.; Toth, I.; Banyai, I.; Kiraly, R.; Brucher, E.; Aime, S.; Sun, X.; Sherry, A. D.; Kovacs, Z. *Inorg. Chem.* **2008**, *47*, 3851.

Table 2. Spectroscopic Properties of [Eu**L**$_P$] and [Tb**L**$_P$] in Aqueous Solutions

	absorption^a λ_{max}/nm (ε/M^{-1} cm^{-1})	τ_{H_2O} ms	τ_{D_2O} ms	ϕ_{H_2O}^{a} %	q^b
L$_P$	300 (17 000)	1.74 ns ^{a}			
[Eu**L**$_P$]	273 (17 500), 280 (17 050), 315 (12 050)	1.50	2.25	2.4	0
[Tb**L**$_P$]	273 (18 200), 280 (17 050), 315 (12 050)	3.28	4.32	37	0

^{a} Measured in 0.01 M TRIS/HCl pH = 7.0. ^{b} Calculated according to ref 13b.

upon complexation, and it is associated to the *cis* to *trans* isomerization of the polyazaaromatic cycles.[26] The lowest energy absorption band is observed at 315 nm in the complexes. When excited in the UV absorption bands, both Eu and Tb complexes exhibited the characteristic emission pattern of the corresponding Ln cations associated to the $^5D_x \rightarrow {}^7F_y$ transitions ($x = 0$, $y = 0-4$ for Eu; $x = 4$, $y = 6-3$ for Tb).[2] When the emission is monitored at the maxima of emission (615 nm for Eu and 545 nm for Tb), the excitation spectra are perfectly superimposed with the absorption spectra, as a result of the ligand-to-metal energy transfer[1] called the antenna effect.[27]

A particularly important property of the complexes of **L**$_P$ is their very long luminescence lifetimes, which are 15 and 19% longer (respectively, for Eu and Tb) than those measured for the complexes of the carboxylated analogue **L**$_C$ (τ = 2.75 and 1.30 ms, respectively, for Tb and Eu in H_2O).[14a] The determination of the hydration number q, the number of water molecules directly linked in the first coordination sphere, was performed according to the conventional procedure developed by Horrocks[13a] using the parameters proposed by Parker et al.[13b] For both complexes, the q values are close to zero, in agreement with a coordination sphere fulfilled by the nonadentate ligand and perfectly shielded from the water environment.

Finally, the luminescence lifetime of the Tb complex was also measured in fetal bovine serum, a biological medium for cell cultures, taken here as a reference medium for the biological media. Because of the very large absorption of the serum itself, it was not possible to directly measure the luminescence quantum yield of the complex in these media (see fluorescence and time-resolved luminescence spectra in Figure S5, Supporting Information). In these conditions, a biexponential fitting of the emission lifetime was necessary, leading to two main components with a long lifetime of 3.50 ms (94% of the total intensity) and a shorter one of 826 μs (4%). It is surmised that the long-lived component, almost identical to that in water, results from unperturbed emission, pointing to an excellent stability of the complex in this medium, with only minor quenching interactions. For the Eu complex (see fluorescence and time-resolved luminescence spectra in Figure S6, Supporting Information), a similar biexponential behavior was observed, but the long-lived component (1.47 ms, 57%) was less important, with 43% of a short-lived species (0.70 ms). This result may be related to the general trend between Eu and Tb, for which the lower energy between the emissive state ($^5D_0$ for Eu at ~17 200 cm^{-1}, $^5D_4$ for Tb at ~20 600 cm^{-1}),[28] and the final states (^7F_J) results in more efficient vibrational quenching processes in the case of Eu.[13] Furthermore, the possibility of redox processes for Eu complexes has to be taken into account.

In contrast to the improved lifetimes, the luminescence quantum yields of the **L**$_P$ complexes are smaller than their analogues with the carboxylated ligand **L**$_C$, especially in the case of Eu (respectively, 13 and 60% for Eu and Tb with **L**$_C$), despite the presence of a similar chromophoric unit. Thanks to the high-resolution emission spectrum obtained for the Eu complex, the methodology developed by Werts and co-workers[29a] was applied to calculate the europium centered luminescence quantum yield, ϕ_{Eu}, and the ligand to metal sensitization efficiency, η_{sens}.[29b]

The high-resolution emission spectrum of the europium complex recorded in 0.01 M TRIS/HCl buffer at pH = 7.0 was decomposed into its five $^5D_0 \rightarrow {}^7F_J$ (J = 0−4) contributions (Figure S7, Supporting Information) and, assuming that the contributions of the weak $^5D_0 \rightarrow {}^7F_{5-6}$ transitions can be neglected,[29a] a radiative lifetime of 5.17 ms was obtained, leading to a 29% Eu centered luminescence efficiency and 8.3% sensitization efficiency. For the Eu complex with **L**$_C$, values of 38 and 34% were reported, respectively, for the metal centered and sensitization efficiencies. According to these results, the lower overall efficiency observed with the phosphorylated complex is mainly the result of a lower sensitization efficiency, which may be attributed to an increase of the distance between the europium cation and the chromophoric unit consecutive to the displacement of the Eu toward the electron donating phosphonate moieties (see DFT calculations below). However, this comparison must be taken with care, as different methods were used to assess the values of η_{sens} and ϕ_{Eu} (Werts method[29] here, hypothesis of nonradiative deactivation at 77 K for [Eu**L**$_C$] in ref 14a). Furthermore, the values reported for the overall luminescence efficiency of [Eu**L**$_C$] are varying from one source[14a] to another.[14b,c]

DFT Modeling. Aiming to obtain information on the solution structure of the lanthanide complexes of **L**$_P$, the [Eu**L**$_P$]$^{5-}$ system was characterized by using DFT calculations at the B3LYP level. In these calculations we have used the effective core potential (ECP) of Dolg et al.[30] and the related [5s4p3d]-GTO valence basis set for the lanthanides, while the remaining atoms were described by using the 6-31G(d) basis set.[31] This ECP includes 46 + 4f^n

(26) (a) Nakamoto, K. *J. Phys. Chem.* **1960**, *64*, 1420. (b) Charbonnière, L.; Mameri, S.; Kadjane, P.; Platas-Iglesias, C.; Ziessel, R. *Inorg. Chem.* **2008**, *47*, 3748. (c) Prodi, L.; Montalti, M.; Zaccheroni, N.; Pickaert, G.; Charbonnière, L.; Ziessel, R. *New J. Chem.* **2003**, *27*, 134.

(27) Alpha, B.; Ballardini, R.; Balzani, V.; Lehn, J.-M.; Perathoner, S.; Sabbatini, N. *Photochem. Photobiol.* **1990**, *52*, 299.

(28) Stein, G.; Würzberg, E. *J. Chem. Phys.* **1975**, *62*, 208.

(29) (a) Werts, M. H. V.; Jukes, R. T. F.; Verhoeven, J. W. *Phys. Chem. Chem. Phys.* **2002**, *4*, 1542. (b) Bünzli, J.-C. G.; Chauvin, A.-S.; Kimb, H. K.; Deiters, E.; Eliseeva, S. V. *Coord. Chem. Rev.* **2010**, *254*, 2623.

(30) Dolg, M.; Stoll, H.; Savin, A.; Preuss, H. *Theor. Chim. Acta* **1989**, *75*, 173.

(31) (a) Regueiro-Figueroa, M.; Esteban-Gomez, D.; de Blas, A.; Rodriguez-Blas, T.; Platas-Iglesias, C. *Eur. J. Inorg. Chem.* **2010**, 3586. (b) Purgel, M.; Baranyai, Z.; de Blas, A.; Rodriguez-Blas, T.; Banyai, I.; Platas-Iglesias, C.; Toth, I. *Inorg. Chem.* **2010**, *49*, 4370.

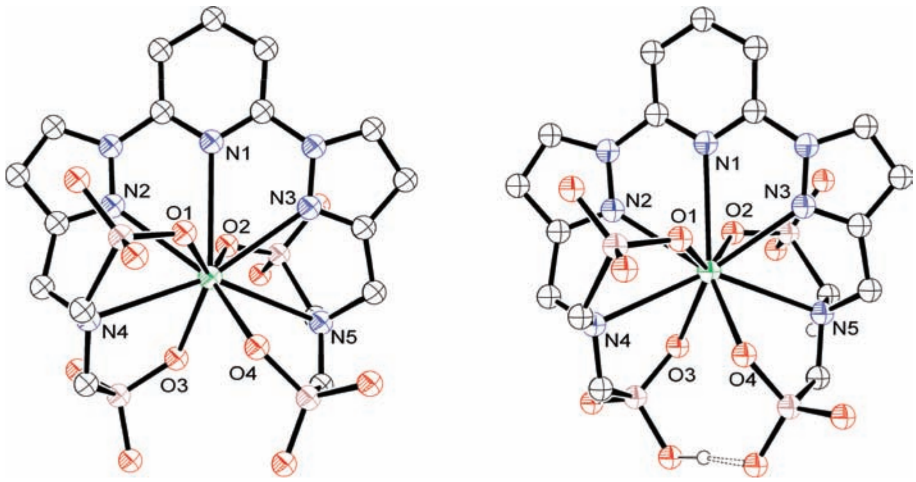

Figure 5. Minimum energy conformations obtained from DFT calculations (B3LYP) in aqueous solution for the $[\mathrm{Eu}\mathbf{L_P}]^{5-}$ and $[\mathrm{Eu}\mathbf{L_P}\mathrm{H}]^{4-}$ systems. Hydrogen atoms, except those involved in hydrogen-bonding interactions, are omitted for simplicity.

electrons of the lanthanide in the core, leaving the outermost 11 electrons to be treated explicitly. Different studies have demonstrated that due to their charge and important structure ordering effect, phosphonate groups have a tendency to induce a second hydration sphere around the metal complexes.[12,21,32] Thus, in our calculations we have taken into account solvent effects (water) by using a polarizable continuum model (PCM).

The minimum energy conformation calculated for the $[\mathrm{Eu}\mathbf{L_P}]^{5-}$ system is shown in Figure 5, while the bond distances of the metal coordination environment are reported in Table 3. According to our calculations, the Eu^{3+} ion is nine-coordinate, being directly bound to the nine donor atoms of the ligand. Two methylenephosphonate groups of the ligand are placed clearly above or below the mean plane of the aromatic tridentate unit of the ligand, while the remaining two methylenephosphonate groups are placed close to that plane. A similar structure was revealed from DFT calculations for the $\mathbf{L_C}$ complexes and confirmed by the analysis of the Yb^{3+}-induced paramagnetic shifts.[17] The conformation adopted by the ligand in $[\mathrm{Eu}\mathbf{L_P}]^{5-}$ implies the occurrence of two helicities: one associated with the layout of the methylenephosphonate arms (absolute configuration Δ or Λ) and the other to the four five-membered chelate rings formed by the binding of the N−CH_2−P−O units (each of them showing absolute configuration δ or λ).[33] The minimum energy conformation calculated for $[\mathrm{Eu}\mathbf{L_P}]^{5-}$ corresponds to the $\Delta(\delta\lambda\delta\lambda)$ [or $\Lambda(\lambda\delta\lambda\delta)$] form.

A comparison of the optimized Eu−donor distances obtained for the $[\mathrm{Eu}\mathbf{L_P}]^{5-}$ and $[\mathrm{Eu}\mathbf{L_C}]^{-}$ systems shows that the replacement of the acetate groups of $\mathbf{L_C}$ by methylenephosphonate groups results in an important lengthening of the distances to the nitrogen atoms of the ligand.[17] This is attributed to a shift of the Eu^{3+} ion to the part of the ligand pocket where the highly negatively charged phosphonate groups are placed, thereby weakening the interaction between the metal ion and the nitrogen atoms of the tridentate aromatic unit of the ligand.

Table 3. Bond Distances (Å) of the Metal Coordination Environment Obtained from DFT Calculations (B3LYP Model) for the $[\mathrm{Eu}\mathbf{L_P}]^{5-}$, $[\mathrm{Eu}\mathbf{L_P}\mathrm{H}]^{4-}$, and $[\mathrm{Eu}\mathbf{L_P}\mathrm{H_2}]^{3-}$ Systems (See Figure 5 for Labeling)

	$[\mathrm{Eu}\mathbf{L_P}]^{5-}$	$[\mathrm{Eu}\mathbf{L_P}\mathrm{H}]^{4-}$	$[\mathrm{Eu}\mathbf{L_P}\mathrm{H_2}]^{3-}$
Eu−N1	3.054	2.891	2.878
Eu−N2	2.747	2.625	2.626
Eu−N3	2.717	2.612	2.604
Eu−N4	2.965	2.912	2.958
Eu−N5	2.905	2.902	2.866
Eu−O1	2.381	2.366	2.479
Eu−O2	2.377	2.361	2.326
Eu−O3	2.345	2.421	2.322
Eu−O4	2.359	2.350	2.399

Different experimental investigations on lanthanide complexes with both acyclic and macrocyclic ligands have revealed partial protonation of phosphonate groups in solution. These protonation constants fall within the range log K = 5.2−8.7,[20,21,25,34] and therefore in most cases protonated forms of the complexes are present in solution around physiological pH. Thus, we characterized the $[\mathrm{Eu}\mathbf{L_P}\mathrm{H}]^{4-}$ and $[\mathrm{Eu}\mathbf{L_P}\mathrm{H_2}]^{3-}$ systems by using DFT calculations. According to our calculations, protonation of the in-plane methylenephosphonate groups is more favorable than protonation of the out-of-plane ones as a consequence of the hydrogen-bonding interaction established between the protonated in-plane methylenephosphonate group and the nonprotonated one (Figure 5, O···O = 2.570 Å, O···H = 1.533 Å, O−H···O = 174.3°). The protonation of the complex provokes important changes in the bond distances of the metal coordination environment (Table 3), while the wrapping of the ligand around the metal ion does not substantially change upon protonation. Indeed, protonation results in an important shortening of the distances to the nitrogen atoms of the aromatic tridentate unit of the ligand and a lengthening of the distance between Eu and the oxygen atom of the protonated phosphonate group. The presence of this hydrogen bonding stabilized protonated state is

(32) Kotek, J.; Lebduskova, P.; Hermann, P.; Vander Elst, L.; Muller, R. N.; Geraldes, C. F. G. C.; Maschmeyer, T.; Lukes, I.; Peters, J. A. *Chem.—Eur. J.* **2003**, *9*, 5899.
(33) (a) Corey, E. J.; Bailar, J. C., Jr. *J. Am. Chem. Soc.* **1959**, *81*, 2620–2629. (b) Beattie, J. K. *Acc. Chem. Res.* **1971**, *4*, 253.
(34) Sherry, A. D.; Ren, J.; Huskens, J.; Brucher, E.; Toth, E.; Geraldes, C. F. G. C.; Castro, M. M. C. A.; Cacheris, W. P. *Inorg. Chem.* **1996**, *35*, 4604.

relevant to the "clipping effect" described by Piguet and other groups.[35] According to our calculations performed on the $[Eu\mathbf{L_P}H_2]^{3-}$ system, the second protonation process involves the protonation of one of the out-of-plane phosphonate groups and it does not have an important effect on the bond distances of the metal coordination environment (Table 3).

Determination of the Thermodynamic Stability Constant. In order to determine the thermodynamic stability constants for the Ln complexes with $\mathbf{L_P}$, we first envisaged pH-potentiometric measurements for one to one metal to ligand mixtures in water (25 °C, 0.1 M KCl). Unfortunately, the precipitation of the complexes at pH below ~4.0 precluded direct stability determination. We then turned our attention toward competition experiments in which increasing amounts of a competing ligand, EDTA, were added to a solution of the Tb complex in 0.01 M TRIS/HCl buffer at pH = 7.4 while monitoring the intensity of the emission peaks of Tb. Particular care was taken to verify first that the solutions have reached their thermodynamic equilibrium (especially for small amounts of added EDTA for which the equilibrium was only reached after few days) and that observed emission was not originating from a possible ternary complex comprising Tb, $\mathbf{L_P}$ and EDTA. For this last point, the luminescence lifetime of Tb was measured and compared to that of the original complex. As no differences were observed, the possibility of a ternary species was discarded. The luminescence decrease was then fitted to the following equilibrium[36] using the SPECFIT program.[24]

$$\mathrm{TbL_P} + \mathrm{EDTA} \leftrightarrow \mathrm{Tb(EDTA)} + \mathbf{L_P} \quad \text{with}$$

$$K_{\mathrm{L_Pcond}} = K_{\mathrm{EDTAcond}} \frac{[\mathrm{EDTA}][\mathrm{TbL_P}]}{[\mathrm{L_P}][\mathrm{Tb(EDTA)}]}$$

in which $K_{\mathrm{L_Pcond}}$ and K_{EDTAcond}, respectively, represent the conditional stability constants for the formation of the Tb complexes with $\mathbf{L_P}$ and EDTA, and $[\mathbf{L_P}]$ and [EDTA] are the sum of the concentrations of the protonated and nonprotonated forms of $\mathbf{L_P}$ and EDTA.[36] The conditional stability constant can then be related to the thermodynamic constant by

$$K_{\mathrm{L_Pcond}} = K_{\mathrm{L_P}} \alpha_{\mathrm{L_P}} \quad \text{with}$$

$$\alpha_{\mathrm{L_P}} = (1 + K_1^{\mathrm{H}}[\mathrm{H}^+] + K_1^{\mathrm{H}} K_2^{\mathrm{H}} [\mathrm{H}^+]^2 + \ldots) \qquad (1)$$

in which the K_i^{H} represents the ith protonation constant of the unprotonated $\mathbf{L_P}^{8-}$ ligand. K_{EDTAcond} was obtained similarly using reported values for the protonation constants.[37] The competition experiment gave us a log K value of 20.4 ± 0.4 (to be compared to 16.18(2) for $\mathbf{L_C}$). Noteworthy, this stability constant is very large and validates the proposed approach of increasing the stability of the complexes by the introduction of phosphonate moieties to obtain complexes stable in biological media.

Conclusions

The replacement of carboxylate functions by phosphonate ones on a bis-aminomethyl functionalized bispyrazolylpyridine platform resulted in a very large increase of the thermodynamic stability for the formation of complexes with Eu and Tb. In addition, the bulkier phosphonate moieties allowed a better shielding of the cations from the solvent molecules and the excited state lifetimes of the complexes are largely improved in water solutions. With the use of fetal bovine serum as a reference medium for biological conditions, the Tb lifetime remained almost identical to that in water, with a value of 3.2 ms of particular interest for bioanalytical applications related to time-resolved detection[3] and multiplexed analysis.[7] In contrast, the luminescence quantum yields of both complexes are less important than their carboxylated analogues. The origin of this decreased efficiency may be related to the larger attraction of the lanthanide cations toward the phosphorylated functions, resulting in a longer distance of the cation from the chromophoric units, as evidenced by DFT modeling of the complexes.

Regarding the very large improvement of the stability obtained with this kind of ligands, our current efforts are directed toward the para-functionalization of the central pyridyl ring, which has been shown to have a very large impact on the photophysical properties of the complexes.[14,15]

Experimental Section

Materials and Methods. Column chromatography and flash column chromatography were performed on silica (0.063−0.200 mm, Merck), silica gel (40−63 μm, Merck), or on standardized aluminum oxide (Merck, Activity II−III). Acetonitrile was filtered over aluminum oxide and distilled over P_2O_5, and K_2CO_3 was flash dried under vacuum prior to use. Other solvents were used as purchased. ^{1}H- and ^{13}C NMR spectra were recorded on Bruker AC 200, Avance 300, Avance 400, or Avance 500 spectrometers working at 200, 300, 400, or 500 MHz, respectively, for ^{1}H. Chemical shifts are given in parts per million, relative to residual protiated solvents.[38] ^{31}P NMR spectra (161.9 MHz) were recorded on the Avance 400 apparatus. IR spectra were recorded on a Nicolet 380 FT-IR spectrometer (Thermo Scientific) as solid samples. Compound **1**[15] and tetraethyliminobis(methanephosponate)[16] were obtained according to literature procedures.

Synthesis of Compound 2. To a solution of compound **1** (282 mg, 0.89 mmol) dissolved in acetonitrile (20 mL), dry K_2CO_3 (333 mg, 2.42 mmol) was added and the mixture was refluxed for 30 min. Tetraethyliminobis(methanephosponate) (160 mg, 0.4 mmol) was added and the mixture was refluxed for 48 h. The remaining K_2CO_3 was removed by filtration and the solvent was evaporated under vacuum. The resulting oily residue was purified by flash chromatography on silica gel (CH_2Cl_2/MeOH, 100/0 to 90/10, R_f = 0.70 at 90/10) to give compound **2** (200 mg, 0.23 mmol) as a yellowish oil (yield: 58%). ^{1}H NMR ($CDCl_3$, 300 MHz): δ 8.49 (d, J = 2.5 Hz, 2H), 7.69−7.95 (m, 3H), 6.54 (d, J=2.5 Hz, 2H), 4.15 (m, (16 + 4)H), 3.23 (d, J=10 Hz, 8H), 1.33 (t, J = 7.2 Hz, 24H). ^{13}C NMR ($CDCl_3$, 75 MHz): δ 152.6, 150.0, 141.2, 127.7, 109.0, 108.6, 62.0 (d, J=7.0 Hz), 52.6 (dd, $^3J_{\mathrm{C-P}}$ = 8.3 Hz, $^1J_{\mathrm{C-P}}$ = 224.0 Hz), 49.0, 16.5 (d, J = 5.8 Hz). ^{31}P NMR ($CDCl_3$, 162 MHz): δ 24.56. ESI$^+$/MS (CH_2Cl_2) m/z = 869.5.

(35) (a) Renaud, F.; Piguet, C.; Bernardinelli, G.; Bünzli, J.-C. G.; Hopfgartner, G. *J. Am. Chem. Soc.* **1999**, *121*, 9326. (b) Charbonnière, L. J.; Ziessel, R.; Guardigli, M.; Roda, A.; Sabbatini, N.; Cesario, M. *J. Am. Chem. Soc.* **2001**, *123*, 2436.
(36) Wu, S. L.; Horocks, W. D. W., Jr. *Anal. Chem.* **1996**, *68*, 394.
(37) Martell, A. E.; Smith, R. M. *Critical Stability Constants*; Plenum Press: New York, 1974; Vol. *1*, p 204.
(38) Gottlieb, H. E.; Kotlyar, V.; Nudelman, A. *J. Org. Chem.* **1997**, *62*, 7512.

Anal. Calcd for $C_{33}H_{59}N_7O_{12}P_4$: C, 45.57; H, 6.84; N, 11.27. Found: C, 46.52; H, 7.05; N, 11.43. IR (cm^{-1}, ATR): ν 3468 (w, O−H), 2980 (w, C_{sp^3}−H), 2907 (w), 1605 (m, C=N), 1585 (C=C aromatic), 1469−1389 (s, C−N), 1259 (m, P=O), 1096−944 (s, P−O), 774 (s).

Synthesis of L_PH_8. Compound **2** (180 mg, 0.21 mmol) was dissolved in 6 N HCl solution (40 mL) and was refluxed for 24 h. The solvent was removed under vacuum and the solid was washed in THF to give $\mathbf{L_P}$ (120 mg, 0.19 mmol) as a pale brown powder (yield: 83%). ^1H NMR (D_2O, 300 MHz): δ 8.68 (d, J = 2.5 Hz, 2H), 7.80−8.15 (m, 3H), 6.85 (d, J = 2.5 Hz, 2H), 4.87 (s, 4H), 3.67 (d, J = 12.5 Hz, 8H). ^{31}P NMR (D_2O, 162 MHz): δ 9.95. ^{13}C NMR (D_2O, 100 MHz): δ 148.7, 144.2, 142.5, 130.0, 110.6, 110.5, 53.2, 51.1 (d, J_{P-C} = 137 Hz). ESI^-/MS (H_2O): m/z = 644.07 (100%); calcd, 644.33 for $\mathbf{L_P}H_7^-$. Anal. Calcd for $C_{17}H_{27}N_7O_{12}P_4\cdot HCl\cdot H_2O$: C, 29.18; H, 4.32; N, 14.01. Found: C, 29.39; H, 4.45; N, 13.82. IR (cm^{-1}, ATR): ν 3417 (w, ν_{O-H}), 1604 (m, $\nu_{C=N}$), 1587 (m, $\nu_{C=CAr}$), 1470 (s, $\nu_{C=N}$), 1388 (m, $\nu_{P=O}$), 1148 (s, ν_{P-O}), 774 (s).

Synthesis of the Complexes. $Na_4[Eu\mathbf{L_P}H]$. Ligand $\mathbf{L_P}$ (20 mg, 31 μmol) was dissolved in water (10 mL), and a solution of $EuCl_3\cdot 6H_2O$ (11.4 mg, 31 μmol) in water (5 mL) was added dropwise. The mixture was heated at 60 °C overnight. A diluted NaOH aqueous solution was added to raise the pH to 7.0, addition of THF resulted in the precipitation of the complex, which was isolated by centrifugation and dried under reduced pressure to give $Na_4[Eu\mathbf{L_P}H]$ (18 mg, 23 μmol) as a white powder. ESI^-/MS (D_2O) m/z = 791.94 (92%), 793.94 (100%); calcd: 791.26 and 793.26 for $[Eu\mathbf{L_P}H_4]^-$. Anal. Calcd for $C_{17}H_{20}EuN_7Na_4O_{12}P_4\cdot 6H_2O$: C, 20.62; H, 3.26; N, 9.90. Found: C, 20.89; H, 3.69; N, 9.82. IR (cm^{-1}, ATR): ν 3372 (w, ν_{O-H}), 1607 (m, $\nu_{C=N}$), 1531 (m, $\nu_{C=CAr}$), 1477 (m, $\nu_{C=N}$), 1389 (w, $\nu_{P=O}$), 1105 (s, ν_{P-O}), 778 (s).

$Na_4[Tb\mathbf{L_P}H]$. Ligand $\mathbf{L_P}$ (20 mg, 31 μmol) was dissolved in water (10 mL) and a solution of $TbCl_3\cdot 6H_2O$ (11.6 mg, 31 μmol) in water (5 mL) was added dropwise. The mixture was heated at 60 °C overnight. A diluted NaOH aqueous solution was added to raise the pH to 7, and addition of THF resulted in the precipitation of the complex, which was isolated by centrifugation and dried under reduced pressure to give $Na_4[Tb\mathbf{L_P}H]$ (20 mg, 25 μmol) as a white powder. ESI^-/MS (D_2O): m/z = 799.9 (100%), 799.96 calcd for $[Tb\mathbf{L_P}H_4]^-$. IR (cm^{-1}, ATR): ν 3374 (w, ν_{O-H}), 1606 (m, $\nu_{C=N}$), 1530 (m, $\nu_{C=CAr}$), 1474 (m, $\nu_{C=N}$), 1389 (w, $\nu_{P=O}$), 1052 (s, ν_{P-O}), 776 (s).

Potentiometric Titrations. Ligand stock solutions were prepared in double distilled water and the exact ligand concentration was determined from the potentiometric titration curves with KOH. Ligand protonation constants were determined by pH-potentiometric titration at 25 °C in 0.1 M KCl. The samples (5 mL) were stirred while a constant Ar flow was bubbled through the solutions. The pH of the titration mixture was adjusted by addition of a known volume of standard aqueous HCl. The titrations were carried out adding a standardized KOH solution with a Methrom 702 SM Titrino automatic buret. A Metrohm 692 pH/ion-meter was used to measure pH. The H^+ concentration was obtained from the measured pH values using the correction method proposed by Irving et al.[39] The protonation constants were calculated from parallel titrations with the program PSEQUAD.[40] The errors given correspond to 1 standard deviation.

Computational Methods. All calculations were performed employing hybrid DFT with the B3LYP exchange-correlation functional,[41] and the Gaussian 09 package (revision C.01).[42] Full geometry optimizations of the $[Eu\mathbf{L_P}]^{5-}$, $[Eu\mathbf{L_P}H]^{4-}$, and $[Eu\mathbf{L_P}H_2]^{3-}$ systems were performed in aqueous solution by using the effective core potential (ECP) of Dolg et al., the related [5s4p3d]-GTO valence basis set for the lanthanides,[30] and the 6-31G(d) basis set for C, H, N, O, and P atoms. No symmetry constraints have been imposed during the optimizations. The default values for the integration grid ("fine") and the SCF energy convergence criteria (10^{-6}) were used. The stationary points found on the potential energy surface as a result of the geometry optimizations have been tested to represent energy minima rather than saddle points via frequency analysis. Solvent effects were evaluated by using the polarizable continuum model (PCM), in which the solute cavity is built as an envelope of spheres centered on atoms or atomic groups with appropriate radii. In particular, we used the integral equation formalism (IEFPCM) variant as implemented in Gaussian 09.[43]

Absorption and Emission Spectroscopy. UV−vis absorption spectra were recorded on a Specord 205 (Analytik Jena) spectrometer. Emission and excitation spectra were recorded in 1 cm^2 quartz Suprasil cells on a Horiba Jobin Yvon Fluorolog 3 spectrometer working with a 450 W Xe lamp in the steady state mode or with a pulsed Xe lamp (fwhh < 4 μs) for time-resolved luminescence experiments. Detection was performed with a Hamamatsu R928 photomultiplier. Luminescence decays were obtained over temporal windows covering at least five decay times and were fitted with the FAST software from Edimburgh Instrument. Luminescence quantum yields were measured according to conventional procedures,[44] with diluted solutions (optical density < 0.05), using $[Ru(bipy)_3]Cl_2$ in nondegassed water (Φ = 2.8%),[45] or rhodamine 6G in ethanol (Φ = 88%)[46] as references, with the necessary correction for refractive index of the media used.[47] Estimated error are ±15%. Hydration numbers, q, were obtained using eq 2, where τ_{H_2O} and τ_{D_2O}, respectively, refer to the measured luminescence decay lifetime (in milliseconds) in water or deuterated water, using $A = 1.2$ and $B = 0.25$[13b] for Eu and $A = 5$ and $B = 0.06$[13b] for Tb (estimated error ±0.2 water molecules).

$$q = A(1/\tau_{H_2O} - 1/\tau_{D_2O} - B) \quad (2)$$

Spectrophotometric absorption and steady state emission titrations were performed according to literature procedures.[48]

Fluorescence (450 W Xe lamp) and time-resolved luminescence spectra (Xe flash lamp, 50 μs delay) of the Eu and Tb complexes in fetal bovin serum were obtained by mixing a volume of the Tb ($c = 4.4 \times 10^{-4}$ M) or Eu ($c = 2.8 \times 10^{-4}$ M)

(39) Irving, H. M.; Miles, M. G.; Pettit, L. *Anal. Chim. Acta* **1967**, *28*, 475.
(40) Zékány, L.; Nagypál, I. In *Computation Methods for Determination of Formation Constants*; Leggett, D. J., Ed. Plenum: New York, 1985; p 291.
(41) (a) Becke, A. D. *J. Chem. Phys.* **1993**, *98*, 5648. (b) Lee, C.; Yang, W.; Parr, R. G. *Phys. Rev. B* **1988**, *37*, 785.
(42) Frisch, M. J.; Trucks, G. W.; Schlegel, H. B.; Scuseria, G. E.; Robb, M. A.; Cheeseman, J. R.; Scalmani, G.; Barone, V.; Mennucci, B.; Petersson, G. A.; Nakatsuji, H.; Caricato, M.; Li, X.; Hratchian, H. P.; Izmaylov, A. F.; Bloino, J.; Zheng, G.; Sonnenberg, J. L.; Hada, M.; Ehara, M.; Toyota, K.; Fukuda, R.; Hasegawa, J.; Ishida, M.; Nakajima, T.; Honda, Y.; Kitao, O.; Nakai, H.; Vreven, T.; Montgomery, J. A., Jr.; Peralta, J. E.; Ogliaro, F.; Bearpark, M.; Heyd, J. J.; Brothers, E.; Kudin, K. N.; Staroverov, V. N.; Kobayashi, R.; Normand, J.; Raghavachari, K.; Rendell, A.; Burant, J. C.; Iyengar, S. S.; Tomasi, J.; Cossi, M.; Rega, N.; Millam, N. J.; Klene, M.; Knox, J. E.; Cross, J. B.; Bakken, V.; Adamo, C.; Jaramillo, J.; Gomperts, R.; Stratmann, R. E.; Yazyev, O.; Austin, A. J.; Cammi, R.; Pomelli, C.; Ochterski, J. W.; Martin, R. L.; Morokuma, K.; Zakrzewski, V. G.; Voth, G. A.; Salvador, P.; Dannenberg, J. J.; Dapprich, S.; Daniels, A. D.; Farkas, Ö.; Foresman, J. B.; Ortiz, J. V.; Cioslowski, J.; Fox, D. J. *Gaussian 09*, revision A.01; Gaussian, Inc.: Wallingford CT, 2009.
(43) Tomasi, J.; Mennucci, B.; Cammi, R. *Chem. Rev.* **2005**, *105*, 2999.
(44) Haas, Y.; Stein, G. *J. Phys. Chem.* **1971**, *75*, 3668.
(45) Ishida, H.; Tobita, S.; Hasegawa, Y.; Katoh, R.; Nozaki, K. *Coord. Chem. Rev.* **2010**, *254*, 2449.
(46) Olmsted, J. *J. Phys. Chem.* **1979**, *83*, 2581.
(47) Valeur, B. In *Molecular Fluorescence*; Wiley-VCH: Weinheim, Germany, 2002; p 161.
(48) Charbonnière, L. J.; Schurhammer, R.; Mameri, S.; Wipff, G.; Ziessel, R. *Inorg. Chem.* **2005**, *44*, 7151.

complexes in TRIS/HCl 0.01 M, pH = 7.0, to a volume of fetal bovine serum (invitrogen).

Acknowledgment. The European Commission is gratefully acknowledged for financial support (7th Framework Programme, HEALTH 2009, NANOGNOSTICS Research Project No. 242264). The authors thank Centro de Supercomputación de Galicia (CESGA) for providing the computer facilities. This research was performed in the framework of the EU COST Action D38 "Metal-Based Systems for Molecular Imaging Applications".

Supporting Information Available: UV−vis vs pH titration experiments of $\mathbf{L_P}$ in water, electrospray mass spectra of $Na_4[Eu\mathbf{L_P}H]$ and $Na_4[Tb\mathbf{L_P}H]$, high-resolution emission spectra of $Na_4[Eu\mathbf{L_P}H]$ in water, ^1H, ^{13}C and ^{31}P NMR spectra of the La^{3+} complex, prompt fluorescence and time-resolved emission spectra of Tb and Eu in fetal bovine serum, and optimized Cartesian coordinates obtained from DFT calculations for the $[Eu\mathbf{L_P}]^{5-}$, $[Eu\mathbf{L_P}H]^{4-}$, and $[Eu\mathbf{L_P}H_2]^{3-}$ systems (12 pages). This material is available free of charge via the Internet at http://pubs.acs.org.